Performance of 3D Forward Looking Sonar for Bathymetric Survey

Heath Henley
Software Engineer
FarSounder, Inc.
Warwick, RI, USA
Email: heath.henley@farsounder.com

Matthew J. Zimmerman
Vice President of Engineering
FarSounder, Inc.
Warwick, RI, USA
Email: matthew.zimmerman@farsounder.com

***Abstract*—Over the past 13 years, the use of 3-dimensional forward-looking sonar (3D FLS) for real-time navigation has been adopted globally by a growing number of vessel operators. More recently, FarSounder started collecting bathymetric data using 3D FLS sonars in Forward Looking Multi-beam (FLMB) mode. Before exploring all of the possible applications of collecting bathymetric data on vessels with an installed 3D FLS navigation system, the accuracy and limitations of this data should first be understood. In this paper, results from two small surveys using a FarSounder 3D FLS in FLMB mode are presented and analyzed. The survey depths are corrected for tide height and compared to NOAA survey data. The average absolute error in depth is found to be 6.6 and 2.2% in the Patience Island and Newport Bridge survey area, respectively. Further, the average survey swath width is computed from the data recorded as ≈9 water depths at ≈6 knots.**

I. Introduction

A. The Development of 3D FLS

Identifying and avoiding navigational hazards in poorly charted or uncharted areas, or areas in which large seasonal changes are common, is a difficult but important task for many commercial, private, and scientific mariners. Since the invention of GPS and improved positioning systems, navigation technology has been improving continuously. Before the development of 3D FLS, a handful of ships used 'searchlight' sonars as an aid in navigation. These systems function in a similar manner to radar, but using sound waves in water instead of electromagnetic waves in air. That is, a directional signal is produced at a specific angle ahead of the vessel, and the returns are recorded. The angle is then changed and the process repeated until the full field of view ahead of the vessel is covered. However, because the speed of sound propagation in water is much less than that of light (or other electromagnetic radiation) in air, these sonar systems are faced with refresh rate limitations that are not present in radar systems. This is especially true at navigationally significant ranges common in today's 3D FLS products. Further, when used in its most common configuration, this technology provides the mariner information about the range and bearing to a potential navigational hazard without obtaining depth information. Obtaining depth information requires a 'searchlight' sonar capable vertical angle selection (unavailable in most 'searchlight' sonars) and requires additional pings. This further increases the time required to generate a full 3D representation of the area ahead of the vessel.

In 2001, FarSounder Inc. developed the technology required to detect not only the range and bearing to potential navigational hazards, but also the depth of the hazard in the water column using a single ping. This means the system is able to refresh the entire 3D field of view on every ping, and is essentially only limited by the time it takes sound to propagate to the longest range (currently 1000m) and back. These technological advances led to the development and release of the first commercially available 3-dimensional FLS system (3D FLS) in 2004.

B. Real-time Depth Detection

A growing number of commercial and private sector vessel operators are adopting 3D FLS as a real-time navigational tool to detect hazards in the water column ahead of the vessel. An added advantage of 3D FLS technology is that the depth of the seafloor ahead of the vessel can also be detected. FarSounder recently released a forward looking multibeam (FLMB) processing technique that allows the bottom to be detected from the 3D FLS data. Prior to the development of this technology, depth measurements with sonar technology required the use of systems oriented down towards the seafloor, eg. multibeam echo sounders. Detecting the depth ahead of the vessel using FLMB allows the user to create a real-time map of the seafloor in-route.

C. Realtime Chart Generation

As more vessels are equipped with 3D FLS for navigation purposes, an opportunity exists to collect and process bathymetric data at a large scale from vessels that otherwise would not obtain this data. This new information would be extremely important to the commercial and scientific community, especially in areas that are uncharted or poorly charted. However, until the recent release of Local History Mapping in version 3.3.0 of FarSounder's SonaSoft™ processing software, 3D FLS technology had never been applied as a tool to collect bathymetric data. It is important to characterize the performance of 3D FLS technology for the collection of bathymetric data in order to explore new applications of 3D FLS and to understand where improvements could be made.

The main objective of this study is to begin to characterize the performance of FarSounder's 3D FLS in FLMB mode as a tool for collecting bathymetric data. A secondary objective of this study is to highlight some of the differences between bathymetric survey data collected using a multibeam echosounder and 3D FLS. Many interesting applications of 3D FLS are emerging ranging from functioning as an aid to exploration and navigation in poorly charted or uncharted areas to improving vessel awareness of transient situations (whales, rocks, seasonal changes) in 'well known' waters. The advantages and utility of using 3D FLS in real-time applications for vessel awareness and navigation purposes are well known. However, the question remains: why would one use a 3D FLS for bathymetric data collection when well understood 2D down facing sonar methods are already in wide use? Most charts are developed from sonar data collected using traditional multibeam technology. Multibeam echo sounder technology in combination with side-scan technology can produce highly detailed pictures and maps of the seafloor below the vessel.

Currently about 50% of the US coastal water with a depth less than 200 m has never been systematically surveyed, and 39% has been designated as "re-survey required" by the International Hydrographic Organization (IHO) [1]. Global survey coverage is even less robust; especially in polar regions, the Caribbean and the Indian and Pacific Oceans. A simple case where the use of 3D FLS is an instance where a survey vessel is entering an uncharted or poorly charted area to survey or re-survey the area. If this vessel were equipped with 3D FLS system, a real-time map of the seafloor ahead of the vessel could be generated and used to identify any unknown navigational hazards (eg. rocks, steep shoals, whales) before transiting into the area and performing a survey using the traditional survey technology (a multibeam echo sounder, for example). This simple example only illustrates one of the many existing and emerging applications of 3D FLS technology. A more detailed review of the current technology and a summary of many other applications and use-cases is presented in Zimmerman and Henley [2]. Further, Wright and Baldauf [3] identify a number of vessel groundings in which the use of a 3D FLS as a navigational aid could have given the crew advance warning of the hazards and allowed them to take corrective action. Russel and Wright [4] highlight some of the differences between data collected using a 3D FLS versus a standard MBES. One difference they illustrate (figure 11, page 54 in Russel and Wright, 2017) is the large degree of ping-to-ping overlap obtained as a function of water depth and speed when a 3D FLS is used to collect bathymetric data. A great deal of overlapping data has exciting implications for improving the accuracy of bathymetric measurements and for increased survey vessel speeds. This new data format presents opportunities for the development of new methods for processing and interpreting the data, and presents a different set of challenges than a traditional MBES.

D. Differences between MBES and 3D FLS for bathymetry

Due to the forward looking orientation of FLS systems, there are a number of differences in the type and amount of data produced per ping. Further, a single bottom detection point in a 3D FLS system is more sensitive than a MBES to uncertainty in measurements obtained from some sensors (eg. pitch) and less sensitive or comparable to others (eg. roll, positioning).

Swath width is a measure of the width (perpendicular to the vessel motion) of seafloor covered by each survey line. Figure 1 illustrates a survey vessel in transit with a traditional multibeam echosounder, the lighter regions indicate where the bottom has been covered by the sonar. As depth increases, the width of the swath increases for a given angular resolution (see figure 1) so is common to present the swath width in units of water depths. Theoretically, a survey vessel with a greater swath width is able to survey a larger area than one with a smaller swath width, because adjacent survey lines can be further apart (assuming the vessels survey at the same speed and the same amount of overlap is required between adjacent survey lines).

In a 3D FLS system operating at normal vessel speeds, there is considerable overlap from one ping to the next. The data produced by the 3D FLS over the length of a survey is a very dense unstructured point cloud consisting of detections from many pings. Size of the overlapping area is a function of the water depth below the transducer, operation mode or characteristics of the product and vessel speed. In general, there is greater uncertainty in any single depth detection obtained by a 3D FLS, compared to a MBES. This is in part due to the geometry of the 3D FLS when detecting bottoms ahead of the vessel. Figure 2 illustrates that a small error in recorded pitch leads to increased error in depth measurement as the surface range increases. Depth soundings from a MBES angled almost directly down is not nearly as sensitive to the error in pitch.

This may seem like a disadvantage for 3D FLS, however because there is a significant amount of overlapping bottom detection from one ping to the next, these errors can be reduced by introducing an averaging method. A simple approach is to take the dense area of unstructured raw detections and reduce the data into a structured grid by averaging neighboring detections into the nearest grid vertex. This approach was applied in this work using a 4 meter grid spacing, and raw detections were averaged into the grid using a normal unweighted average. In the future, more sophisticated methods could be used to weight detections as they are added to the grid vertex based on some other parameters, for example the Office of Coast Survey at NOAA suggests that angle from nadir, depth threshold, and total propagated uncertainty can be used [6]. As another possible data quality improvement, grid vertices could be removed from the dataset algorithmically based on a chosen criteria, for example if they have a depth variance that is greater than a chosen cutoff or if there are too few depth points included into the vertex. The later approach

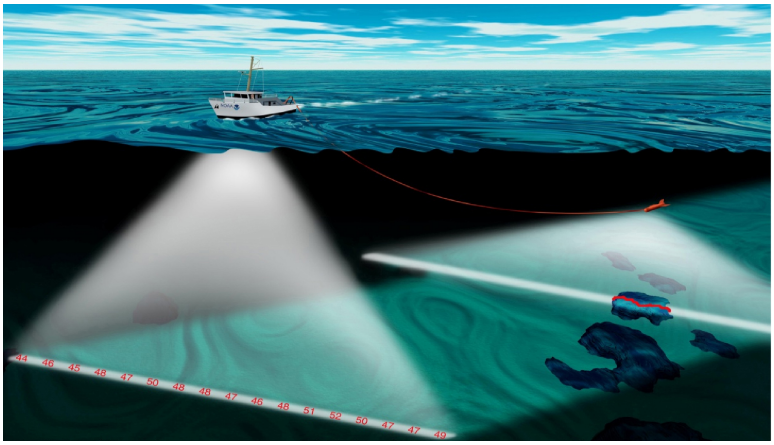

Fig. 1. Swath width illustration.NOAA Image Credit [5]

is applied in the Shallow Survey 2018 Common Data Set requirements (eg. in their case, each 2 m grid must contain at least 9 sounding points). Further, a more sophisticated algorithm, such as the CUBE (Combined Uncertainty and Bathymetric Estimator) algorithm could be implemented [7].

II. Procedure

Two surveys were performed in the Narragansett Bay to collect bathymetric data for this study. The FarSounder sonar was temporarily installed on University of Rhode Island's R/V Cap'n Bert. The processed sonar depth points were corrected for tide height, sensor positioning on the ship (GPS, Transducer Module, etc.), and vessel orientation (eg. roll/tilt) in real-time. Note that in this work, no calibration patch tests were performed to correct of biases in roll, pitch and heading measurements, heave was not measured or considered, and an iso-velocity sound speed profile of 1,500 meters per second was assumed. For reasons discussed previously, a structured grid with 4 meter spacing was generated by averaging raw neighboring detections into the nearest grid vertex.

A. Survey areas

Figures 3 and 4 show the survey area of Patience Island survey route and the Newport Bridge survey route, respectively. The screenshots were captured directly from the chart viewer display inside FarSounder's SonaSoft™ user interface software, with zoomed insets added afterward.

B. Temporary Sonar Installation

For this study, FarSounder sonars were temporarily installed on the R/V Cap'n Bert, a 16 meter research vessel operated by University of Rhode Island. The Transducer Module is temporarily attached to the bow of the M/V Cap'n Bert using an aluminum pole mount (see figure 5). The vessel speed was kept under 6 knots to avoid excess stress on the pole mount.

The Transducer Module sits about 0.9 meters below the surface of the water when installed on the R/V Cap'n Bert's bow mount. A Furuno SC-30 GPS compass was also temporarily installed to provide position, speed over ground, heading, and rate of turn information. The locations of the GPS compass unit and the Transducer Module relative to the ships datum were used to determine the physical position of the recorded sonar data in real-time.

TABLE I
NOAA Survey Reference Data

NOAA Survey	Year	Reference	Resolution (M)
H11930	2011	[8]	4
H11988	2008-2009	[9]	4
F00522	2006	[10]	0.75

C. NOAA Survey Data

Quantitatively evaluating the performance of FarSounder's 3D forward looking sonar for real-time bathymetric survey applications necessarily requires 'ground truth' or reference data for comparison. For the purposes of this study, survey data gathered by NOAA using standard multibeam sonar survey technology is treated as 'ground truth'. The data was obtained as bathymetric attributed grid (BAG) files from NOAA. Table I gives some details for the NOAA surveys referenced in this work.

III. FarSounder 3D FLS Performance for Realtime Bathymetric Survey

All of the sonar data collected for this study was processed by FarSounder's SonaSoft™ software. Survey data was downloaded from NOAA for use as a reference in the areas of interest. Bottom detections from the FLS were corrected for the current tide height in real time using predictions from the nearest tidal database in the C-MAP Professional+ database. In an effort to evaluate the performance of real-time data collection, we refrain from (1) using actual reported tide heights, (2) any other filtering or manual outlier removal. Note that using the actual tidal recorded tide heights and by applying some simple outlier removal, the error can be further reduced (see table II).

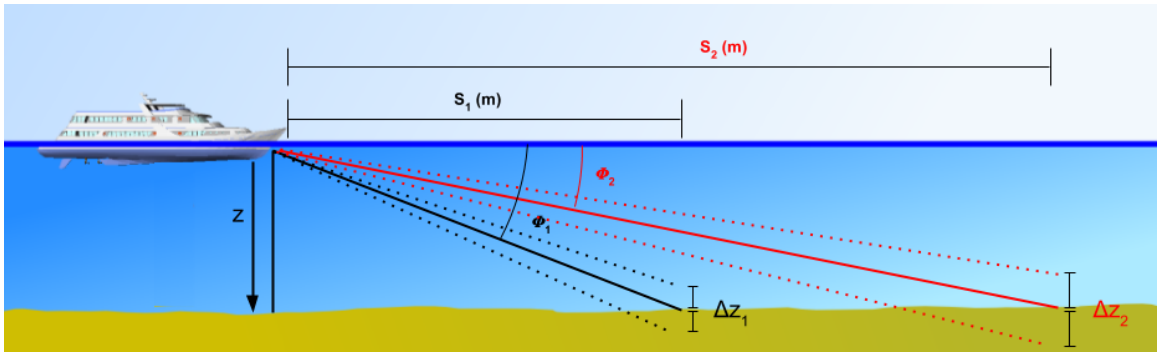

Fig. 2. Deviation in detected depth at two vertical angles ϕ_1 and ϕ_2 due to pitch uncertainty. The solid lines represent the vertical angles (ϕ_1 and ϕ_2) while the dashed lines represent ϕ_1 and ϕ_2 $\pm\Delta\phi$

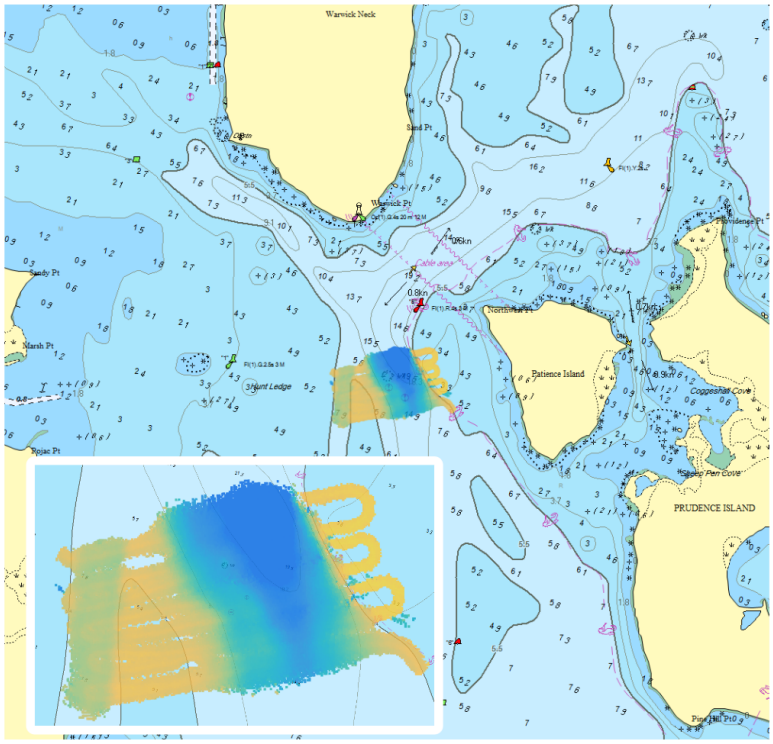

Fig. 3. Patience Island survey area overlay in SonaSoft^{TM}

In this work, the average absolute deviation (AADP) (eq. 1) was used to compute the relative error between the FarSounder and NOAA survey results. Note this accuracy measure is also commonly called the mean absolute percentage error (MAPE).

$$AADP = \frac{100}{N}\Sigma_{i=1}^{N}\left|\frac{(x_i - x_{i,ref})}{x_{i,ref}}\right| \quad (1)$$

Where N represents the number of data points and x represents depth in this case. The subscript 'ref' denotes a reference datapoint. As previously mentioned, 3D FLS generates a dense cloud of points ahead of the vessel. These points are averaged into a spatially structured (4 meter grid spacing in this case) grid. The average depth value at a given grid vertex is then compared with the nearest NOAA reference value according to equation 1. A running count and some statistics are computed at each grid vertex as points are added, including the average and variance in depth, signal strength, and target strength. The uncertainty in the AADP (equation 1) due to the the standard deviation of the average depth at the FarSounder grid vertex, and the vertical uncertainty from the NOAA BAG data was estimated using a standard error propagation procedure.

A. Tide Correction

The C-MAP Professional+ database provides nautical data for FarSounder's SonaSoft^{TM} software, including charts, locations of navigational hazards, tidal stream and tidal height predictions. NOAA collects tidal height data from many tidal stations located throughout the United States. In addition to collecting tide height measurements, NOAA produces predictions of the tide height at any given time, for a chosen station.

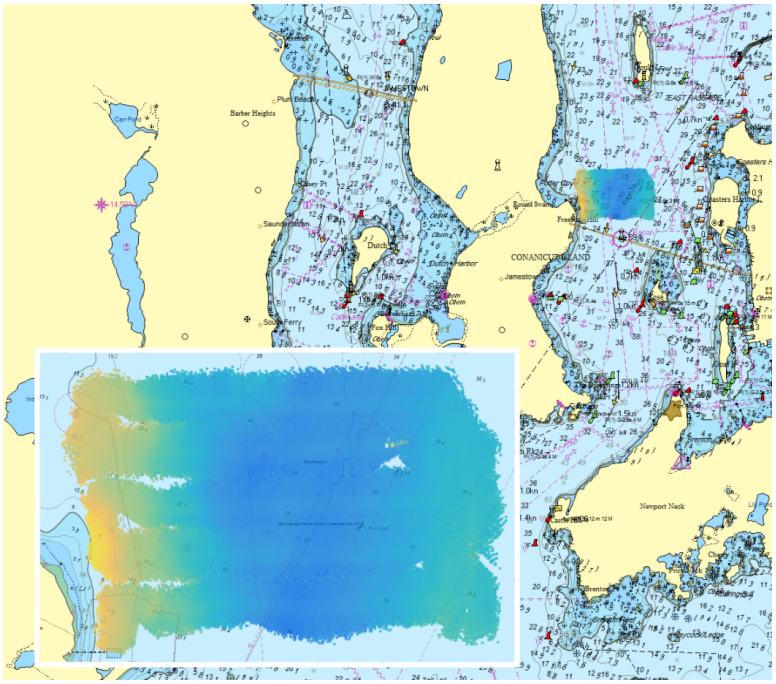

Fig. 4. Newport Bridge survey area overlay in SonaSoft™

Fig. 5. Aluminum bow mount on the Cap'n Bert.

Figures 6 and 7 plot the NOAA predicted and measured tide height, along with the C-MAP predicted value for the relevant survey areas over the time of the survey. The C-MAP predicted tide height over both the survey areas and times was closer to the measured values than the NOAA predicted values (see figures 6 and 7, dash-dot line versus dashed line).

Obviously, the most accurate tide station based correction that could be applied to the bathymetric data would be the actual measured values (solid lines in figures 6 and 7). However, this data is not readily available for real-time applications. Thus, to simulate a real-time bathymetric survey, the C-MAP predicted value is used to correct the sonar bottom detections to a datum of mean low-low water (MLLW). Note that more accurate tide height information could be obtained by interpolating in position between the surrounding tide station predictions, or using the vertical component of Real-Time Kinematic (RTK) GPS sensors [11].

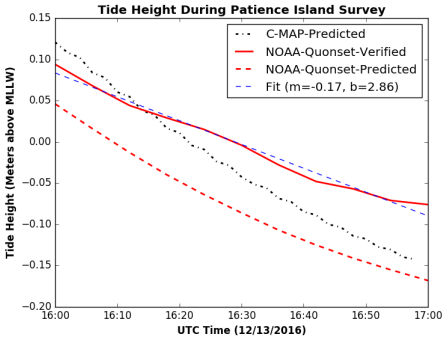

Fig. 6. Predicted tide heights (NOAA and C-MAP) and measured tide heights (NOAA) for the tide station closest to the Patience Island survey area.

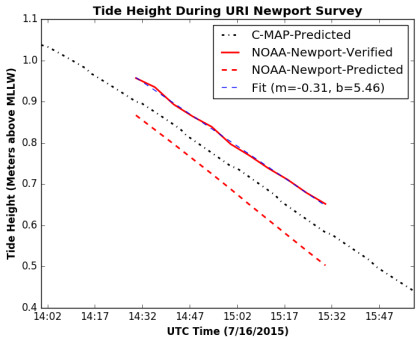

Fig. 7. Predicted tide heights (NOAA and C-MAP) and measured tide heights (NOAA) for the tide station closest to the Newport Bridge survey area.

B. Survey Results

Table II details the overall statistics for the comparison between FarSounder's survey results and the reference data downloaded from NOAA. Examples marked "realtime" in Table II indicate that the survey data was recorded by FarSounder and corrected for tide height in real-time and that no outlier removal, filtering, or other post-processing was performed before making the comparison to NOAA data. For examples marked as "processed", a more traditional survey processing approach was applied in which outliers in the data were manually removed and the tide height correction was applied using the actual measured tide heights from the closest NOAA tide station. A linear line of best fit was used to model the NOAA measured tide heights over the short time of the surveys (see figures 6 and 7). The cutoff for classification of a data point as an outline was arbitrarily chosen as the value of percent error such that 99.7% of the data fall below the cutoff.

Figures 8a and 8b show the FarSounder real-time survey data versus the NOAA data over the respective survey areas, while the post-processed data for the same FarSounder surveys is displayed in figures 8c and 8d. Introducing a more accurate measure of the tide height and removing outliers reduces the average absolute deviation by 1.7% and 0.1% in the Patience Island survey and Newport Bridge survey, respectively.

TABLE II
OVERALL COMPARISON RESULTS

Example	AAD%	σ_N	N_d
Patience Island (Realtime)	6.6 (0.2)	14.7	4448
Newport Bridge (Realtime)	2.4 (0.04)	3.4	43021
Patience Island (processed)	4.9 (0.2)	3.8	4407
Newport Bridge (processed)	2.3 (0.04)	2.43	42839

C. Swath width

The swath width of the FarSounder sonars was calculated as a function of speed for both the Patience Island and Newport Bridge survey datasets. Averaging the swath width measurements for all data at ≈6 knots over both surveys resulted in an average swath width of 9±3 water depths (below Transducer Module), or ≈4.5 water depths off of each side.

During data acquisition, vessel speed was kept below 6 kn to limit the amount of stress on the bow mount. To estimate the swath width at higher speeds, the raw sonar data was downsampled by an appropriate factor and reprocessed. For example, to simulate moving at approximately twice the speed, every other ping was discarded and the data was reprocessed. Note that this approach does not account for any changes that may be observed in roll/tilt, increased vessel engine RPM, and draft if the vessel were actually moving at an increased speed. These factors may have some effect on the error characteristics of the processed results when compared to reference data. However the effect on the swath width and overall survey footprint should be negligible. Note that the width of the swath was measured perpendicular to the motion of the vessel, and the start and end points of the measurement were determined visually as the start/end of 100% coverage. Calculated swath width as a function of depth in figure 9a at constant speed, and depth normalized swath width is presented as function of vessel speed in Figure 9b for both surveys.

Figure 9a suggests that up to about 15 meters water depth at 6 knots, the available swath width is about 10 water depths. However, in the deeper water encountered in the Newport Bridge survey dataset, the average swath width is only about 7 water depths at 6 knots. In a 3D FLS system, there is a significant amount of overlap from one ping to the next. As vessel speed increases, the amount of overlap in the footprint or 'field of view' of each ping decreases, which leads to a decrease in 100% coverage swath width as a function of speed. However, the amount of overlap between the footprints of consecutive pings may make the 100% coverage swath width of a 3D FLS system less dependent on vessel speed than a typical multibeam echo sounder.

D. Real-time Bathymetry and IHO Survey Standards

General standards for the accuracy of bathymetric survey data are defined by the International Hydrographic Organization (IHO). Four separate orders are defined by the IHO with different tolerances and requirements. They are Special order, Order 1a, Order 1b and Order 2. As Order 2 is only

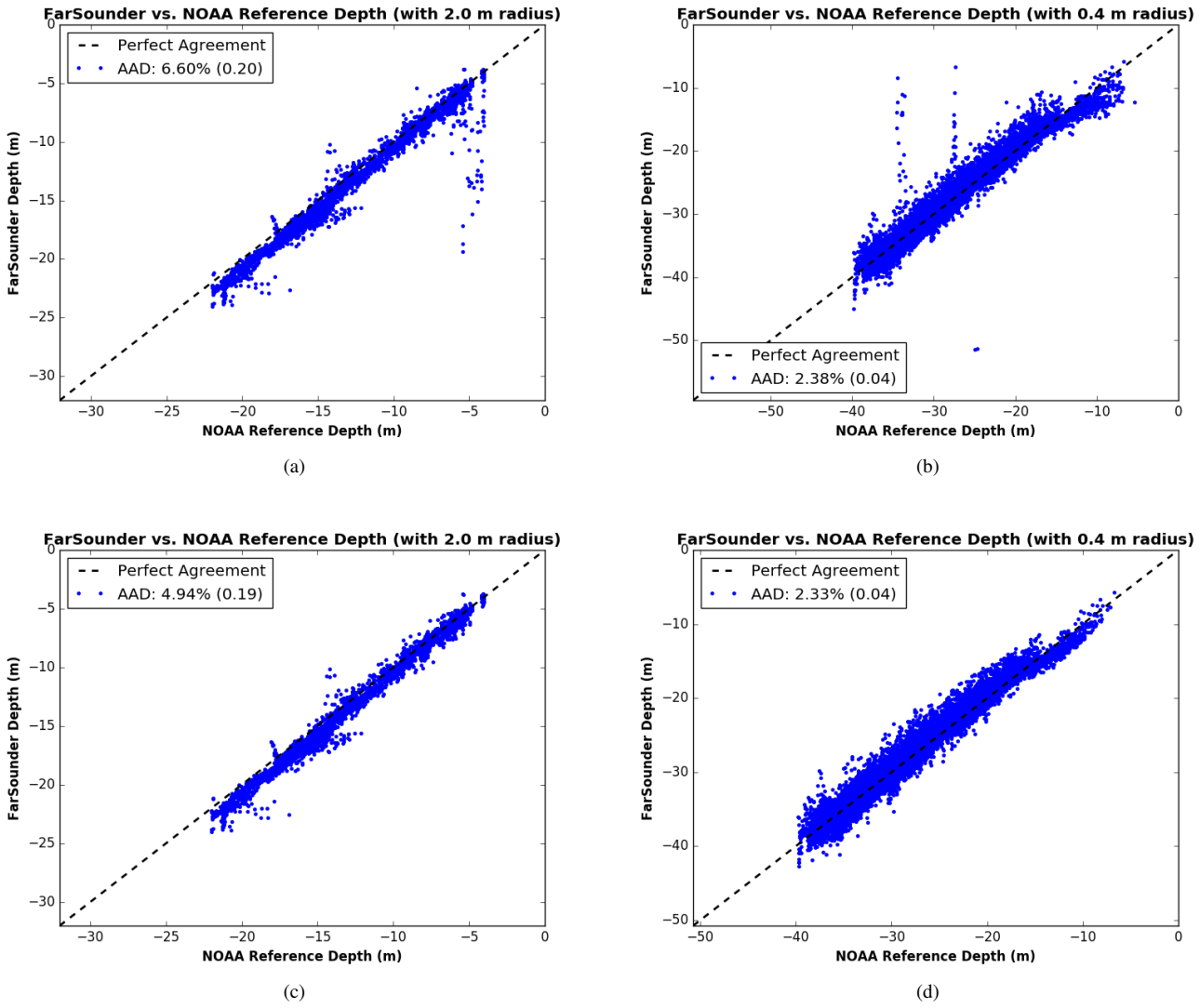

Fig. 8. Top: FarSounder real-time depth values versus the NOAA reference values for the Patience Island survey (a, top left) and the Newport Bridge survey (top right, b). Bottom: post-processed depth value versus NOAA reference data for the Patience Island (c, bottom left) and Newport Bridge (d, bottom right) surveys.

relevant for waters deeper than 100 m it was not considered here [12]. Special order contains the most stringent criteria for survey data as it is intended for water less than 40 m deep and in areas where 'under keel clearance is critical'. Orders 1a and 1b share the same vertical uncertainty requirements, but are differentiated by feature detection criteria (eg. Order 1a requires the detection of cubic features $>$ 2 m in depths up to 40 m, while Order 1b does not). The red dashed and solid lines in figure 10 represent the minimum allowed vertical uncertainty criteria defined by IHO for Special Order and Order 1a/b as a function of depth, respectively. Figure 9 also plots two standard deviations of the average depth at each 3D FLS grid vertex used in the comparison. The inset in figure 10 is a histogram of point density, or a 'heat map', with a logarithmic frequency scale. From figure 10, it is clear that there is notable variance in of the 3D FLS 48,000 gridded depth points used in this study. However, the highest concentration of data points (see figure 10 inset) are either below or near the IHO standard criteria, especially the Order 1a/b criteria.

Though the overall vertical uncertainty (as estimated using the twice the grid vertex standard deviation in depth) in the 3D FLS bathymetric survey data is not all below the IHO requirements for Special Order or Order 1a/b currently, there are a number of improvements that can be made to collection and processing of the data to improve accuracy in the future. For instance, sound speed profile corrections could be applied, the roll and pitch sensors could be calibrated using patch test prior to collecting survey results, doppler corrections could be applied, RTK GPS could be used to obtain more accurate information about the current tidal height, and additional filtering algorithms could be implemented as described previously.

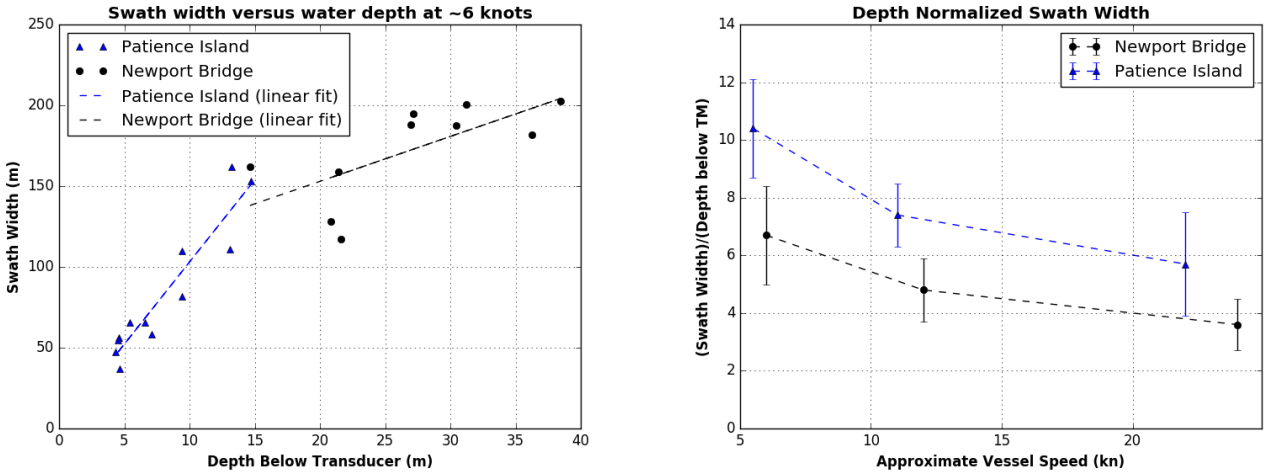

(a) (b)

Fig. 9. Left (a): Swath width as a function of water depth at a constant vessel speed of ≈6 kn for both the Patience Island (blue triangle) and Newport Bridge (block circle) datasets.Right (b): water depth (below transducer module) normalized swath width as a function of approximate vessel speed for both the Patience Island (blue triangle) and Newport Bridge (block circle) datasets.

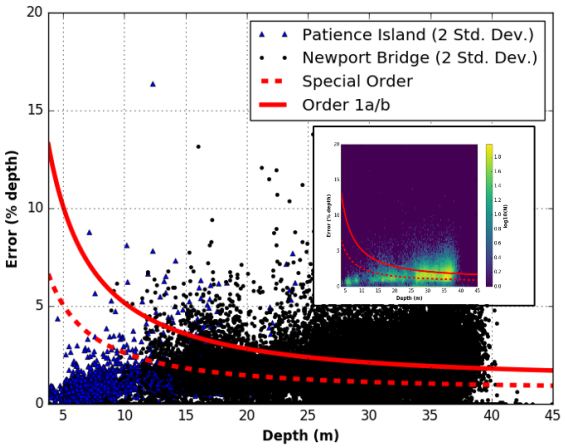

Fig. 10. FarSounder 3D FLS grid vertex standard deviation as function of depth for both survey datasets. Inset: histogram showing point density on a logarithmic scale.

In addition, a base value of the total propagated uncertainty (TPU) will be calculated for the data collection system using manufacturer uncertainty specifications of all of the sensors in the system, uncertainty in sensor positioning relative to the vessel datum, and uncertainty in the tide height measurements or predictions.

IV. Conclusion

Many promising applications exist for today's 3D forward-looking sonar technology, including collection of bathymetric data. Performance characteristics and limitations should be well understood to guide the ongoing development of 3D FLS applications involving collection of bathymetric survey data. In this study, the accuracy of FarSounder's 3D FLS sonar in forward looking multi-beam (FLMB) mode for the collection of bathymetric survey data in real-time was evaluated using the results of two example surveys in Rhode Island's Narragansett Bay. Survey results reported by NOAA were used as standard of comparison to compute all error metrics. Tide height prediction was obtained in real-time from the C-MAP Professional+ database and used to correct to FLMB data to MLLW for comparison to NOAA data. Survey data processed in real-time with no outlier removal or other corrections resulted in an AAD % of 6.6 and 2.3 for the Patience Island and Newport Bridge datasets, respectively. At 6 knots, the average swath width was ≈ 9 water depths overall which is comparable to a standard 2D down-looking multibeam sonars. Finally, the distribution of the percent error between the 3D FLS data and the NOAA data and the uncertainty in the 3D FLS data was compared to IHO survey standards. Though the overall uncertainty in the 3D FLS data is not below IHO survey requirements, a significant portion of the dataset is. Suggesting that with improvements in the processing and collection of the data, 3D FLS systems will be capable of providing survey data in compliance with Special Order and Order 1a/1b requirements.

References

[1] IHO, "IHO Publication C-55 - Status of Hydrographic Surveying and Charting Worldwide," International Hydrographic Organization, Tech. Rep., 2017. [Online]. Available: https://www.iho.int/iho_pubs/CB/C-55/c55.pdf

[2] M. Zimmerman and H. Henley, "Applications of Today's 3D Forward Looking Sonar for Real-time Navigation and Bathymetric Survey," in *OCEANS 2017*, 2017.

[3] R. G. Wright and M. Baldauf, "Hydrographic Survey in Remote Regions: Using Vessels of Opportunity Equipped with 3-Dimensional Forward-Looking Sonar," *Marine Geodesy*, vol. 39, no. 6, pp. 439–457, 2016. [Online]. Available: https://www.tandfonline.com/doi/full/10.1080/01490419.2016.1245226

[4] I. Russel and R. G. Wright, "NAVIGATION SONAR: MORE THAN UNDERWATER RADAR Realizing the full potential of navigation and obstacle avoidance sonar," *International Hydrographic Review*, no. May, pp. 41–60, 2017.
[5] NOAA, "Bermuda: Search for Deep Water Caves," 2009. [Online]. Available: http://oceanexplorer.noaa.gov/explorations/09bermuda
[6] ——, "Field Procedures Manual," *National Oceanic and Atmospheric Administration*, no. April, pp. 1–333, 2011.
[7] B. Calder, "Automatic statistical processing of multibeam echosounder data," *The International Hydrographic Review*, vol. 4, no. 1, pp. 53–68, 2003.
[8] NOAA, "NOAA Survey H11930," 2011. [Online]. Available: https://www.ngdc.noaa.gov/nos/H10001-H12000/H11930.html
[9] ——, "NOAA Survey H11988," 2008. [Online]. Available: https://www.ngdc.noaa.gov/nos/H10001-H12000/H11988.htm
[10] ——, "NOAA Survey F00522," 2006. [Online]. Available: https://www.ngdc.noaa.gov/nos/F00001-F02000/F00522.htm
[11] P. Sanders, "RTK Tide Basics," *Hydro International*, 2008. [Online]. Available: https://www.hydro-international.com/content/article/rtk-tide-basics-9
[12] IHO, "IHO Publication S-44: Standards for Hydrographic Surveys," International Hydrographic Organization, Tech. Rep., 2008. [Online]. Available: http://iho.int/iho_pubs/standard/S-44_5E.pdf